Supporting Information

NIR-Responsive Reversible Phase Transition of Supramolecular Hydrogels for Tumor Treatment

Ting Zhang,[a] Zhiyu Liu,[c] Hüsnü Aslan,[d] Chunhua Zhang*[a] and Miao Yu*[b]

a MIIT Key Laboratory of Critical Materials Technology for New Energy Conversion and Storage, School of Chemistry and Chemical Engineering, Harbin Institute of Technology, P. O. Box 1254, Harbin, 150001, P. R. China. Email: zhangchunhua@hit.edu.cn
b School of Chemistry and Chemical Engineering, Harbin Institute of Technology, Harbin, 150001, P. R. China. Email: miaoyu_che@hit.edu.cn
c Department of Chemistry and Biochemistry, University of California, Los Angeles, Los Angeles, California, 90095, USA
d Interdisciplinary Nanoscience Center (iNANO), Aarhus University, The iNANO House, DK-8000 Aarhus, Denmark, Aarhus, DK 8000

Contents

1. Synthesis of the compounds

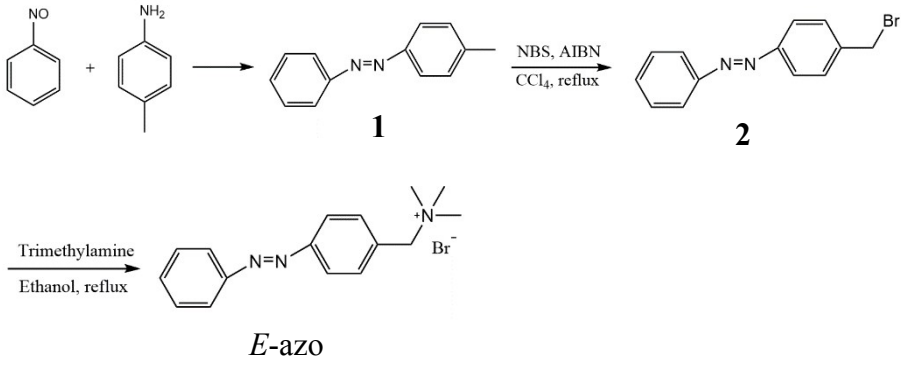

Scheme S1 Synthetic routes of compound **1**, **2** and *E*-azo.

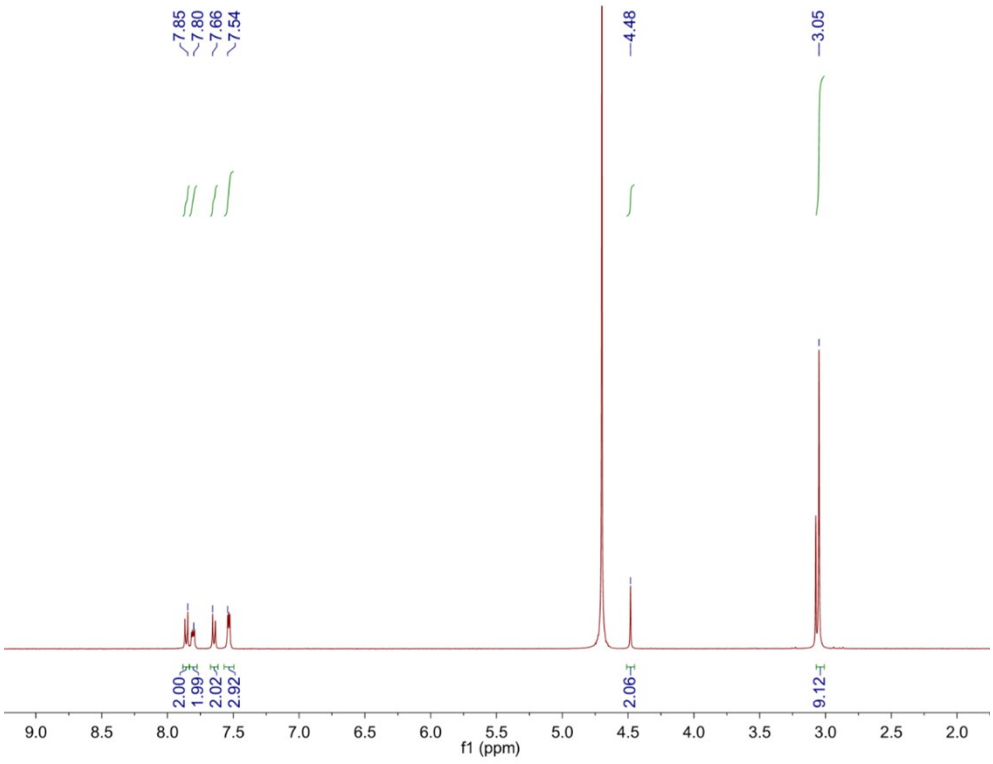

Fig. S1 ^{1}H NMR spectrum (400 MHz, D_2O) of compound *E*-azo at 298 K.

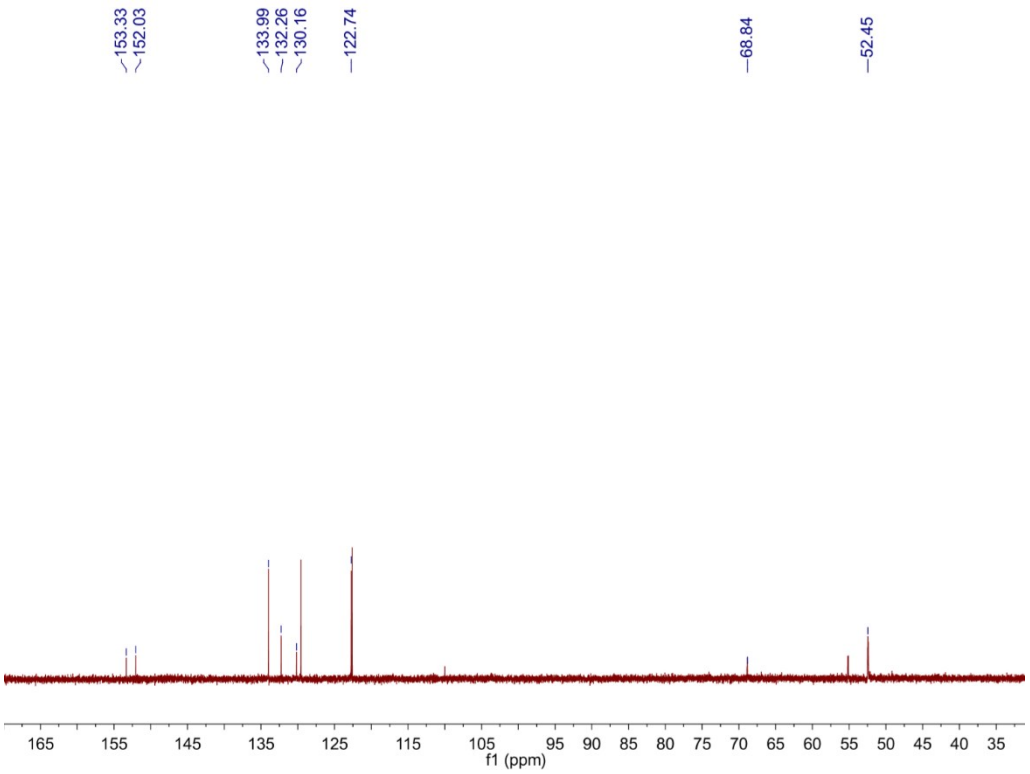

Fig. S2 ^{13}C NMR spectrum (400 MHz, D_2O) of compound *E*-azo at 298 K.

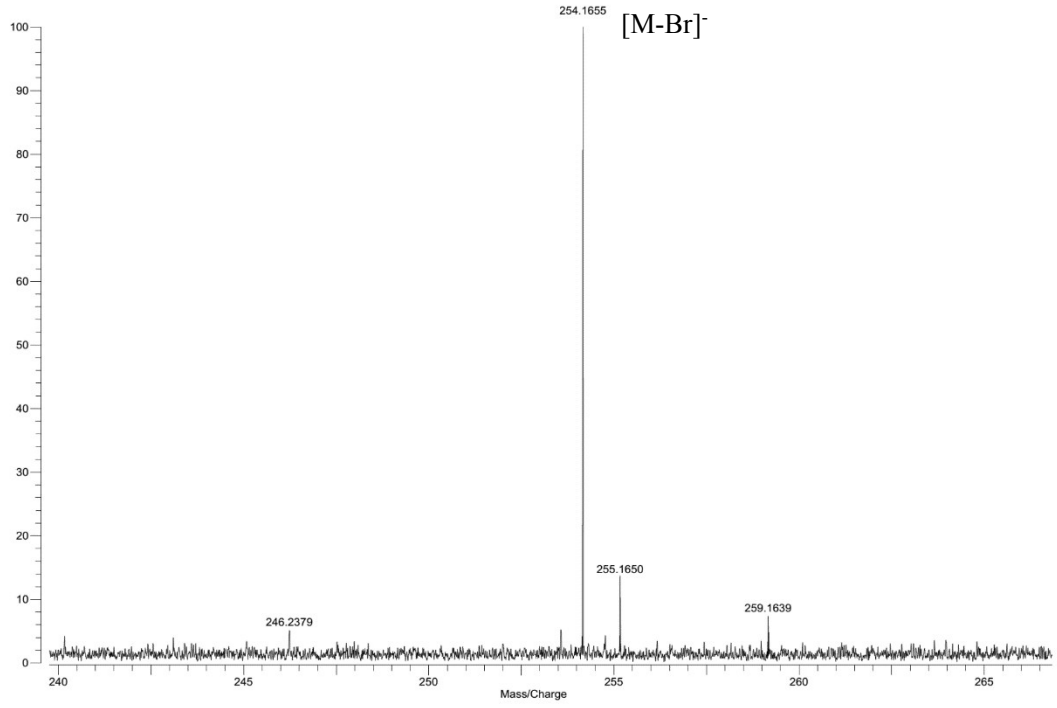

Fig. S3 The ESI-MS spectrum of compound *E*-azo.

2. Characterizations of the products

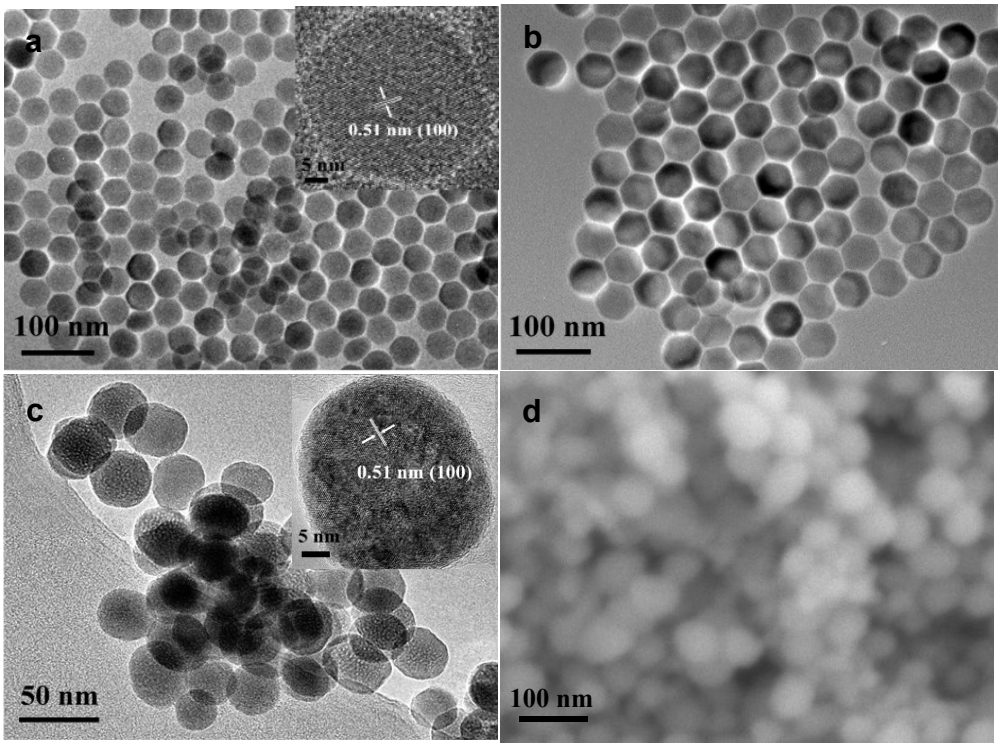

Fig. S4 (a) TEM image of the $NaYF_4$:Yb,Tm, Inset: HRTEM image of $NaYF_4$: Yb, Tm; (b) TEM image of $NaYF_4$:Yb,Tm@$NaYF_4$ (UCNP), (c) TEM and (d) SEM image of the UCNP@α-CD, Inset: HRTEM image of UCNP@α-CD.

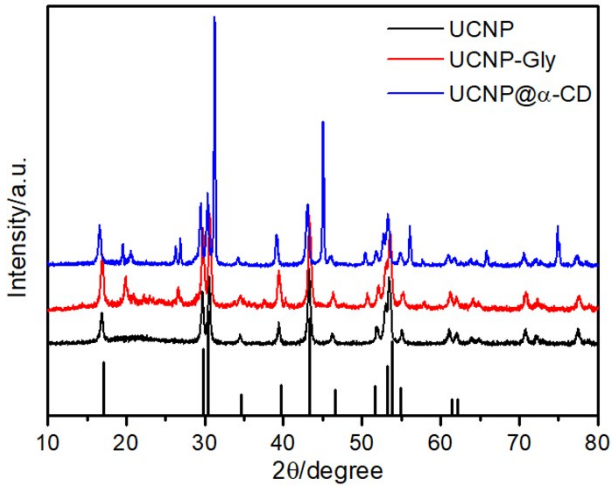

Fig. S5 Powder X-ray diffraction (XRD) pattern of UCNP, UCNP-Gly, UCNP@α-CD and the calculated line pattern for the hexagonal $NaYF_4$ phase.

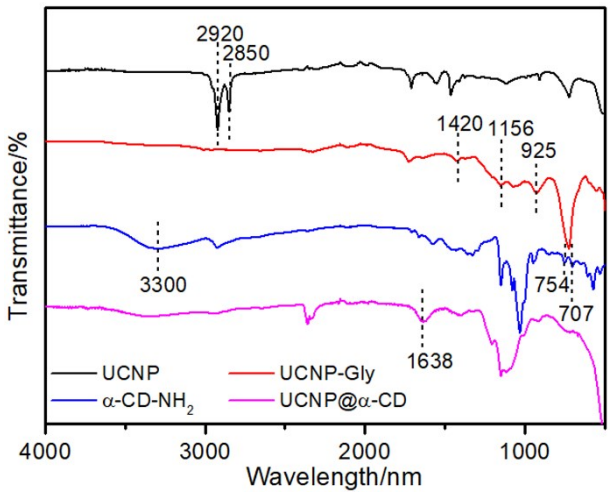

Fig. S6 The FITR spectrum of UCNP, UCNP-Gly, α-CD-NH_2, UCNP@α-CD.

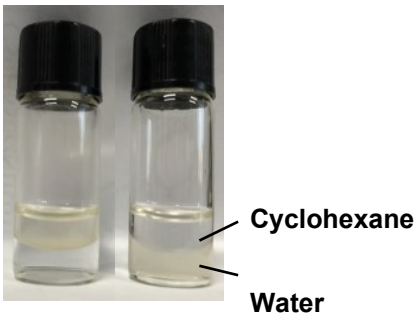

Fig. S7 Digital photos of UCNP (left) and UCNP@α-CD (right) dissolved in cyclohexane and water, respectively.

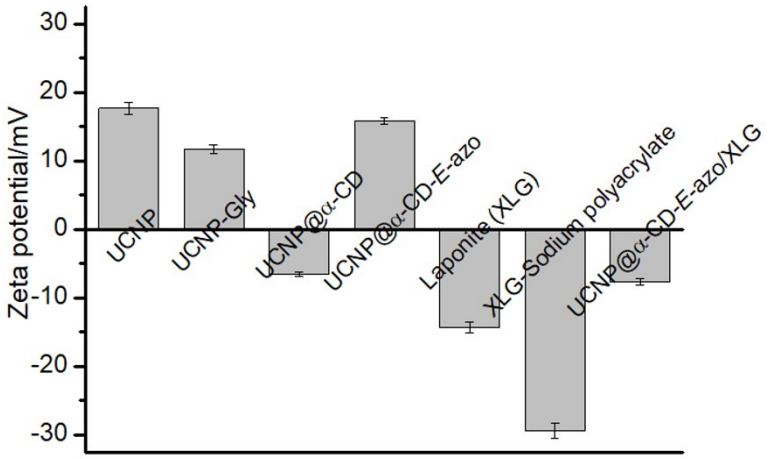

Fig. S8 The zeta potentials of UCNP, UCNP-Gly, UCNP@α-CD, UCNP@α-CD-*E*-azo, Laponite(XLG), XLG-Sodium polyacrylate, UCNP@α-CD-*E*-azo/XLG.

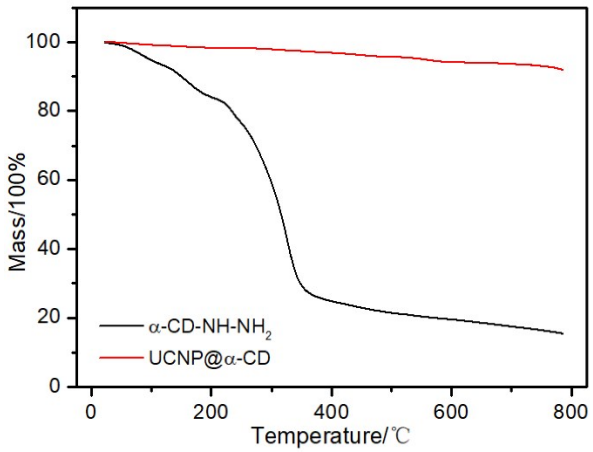

Fig. S9 TGA analysis of α-CD-NH-NH_2 and UCNP@α-CD.

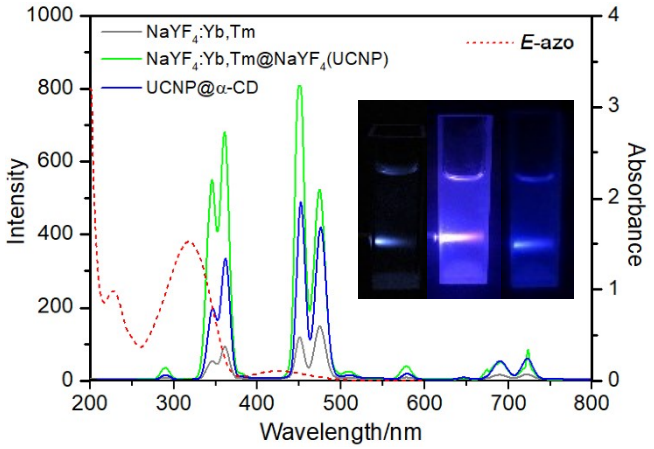

Fig. S10 Emission spectra and corresponding digital photos of $NaYF_4$:Yb,Tm, $NaYF_4$:Yb,Tm@$NaYF_4$ (UCNP) and UCNP@α-CD. Samples were dispersed in aqueous solution at the same concentration. The red dotted line is UV-Vis absorption spectra of *E*-azo.

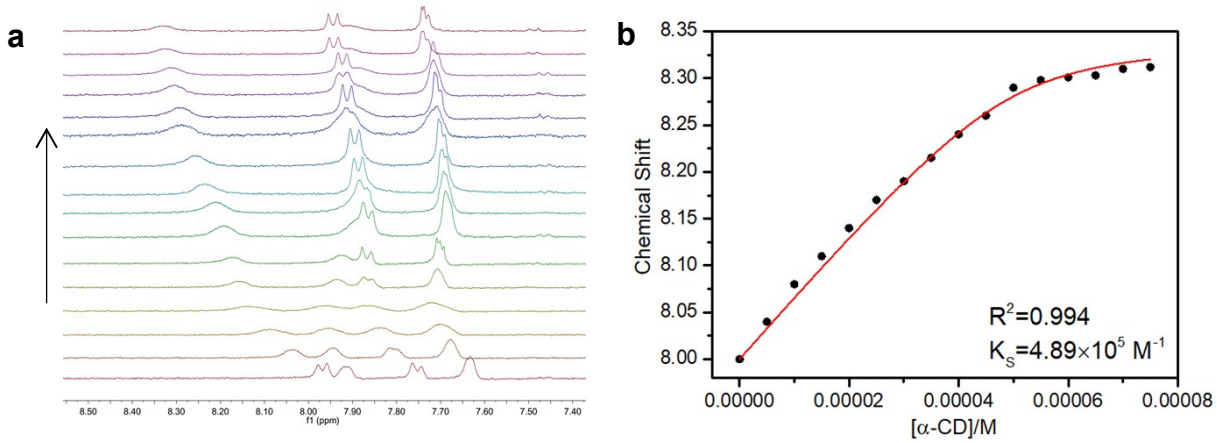

Fig. S11 (a)^{1}H NMR spectral changes of Guazo upon addition of α-CD at 25°C ([azo] = 0.05 mM, [α-CD] = 0-0.75 mM, respectively), (b) The nonlinear least-squares analysis of the differential chemical shifts (δ) to calculate binding stability constant (K_S).

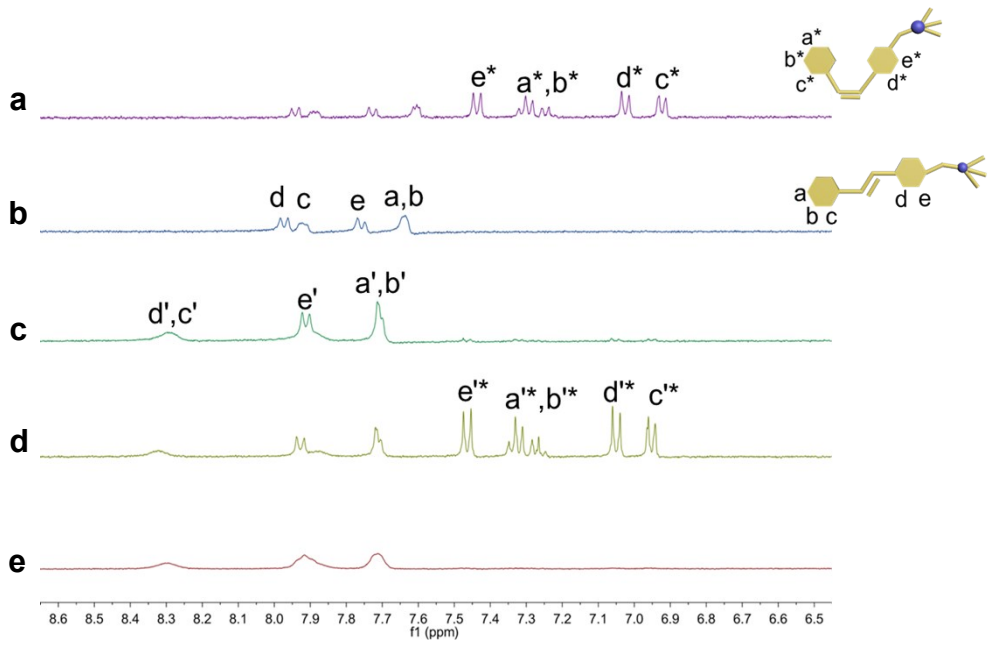

Fig. S12 ^{1}H NMR spectra of (a) 1.00 mM *E*-azo after irradiation at 365 nm for 10 min, (b) 1.00 mM *E*-azo, (c) 1.00 mM α-CD-*E*-azo, (d) after irradiation at 365 nm for 10 min (e) and then after further irradiation at 420 nm for 1 min. (400 MHz, D_2O, 298K).

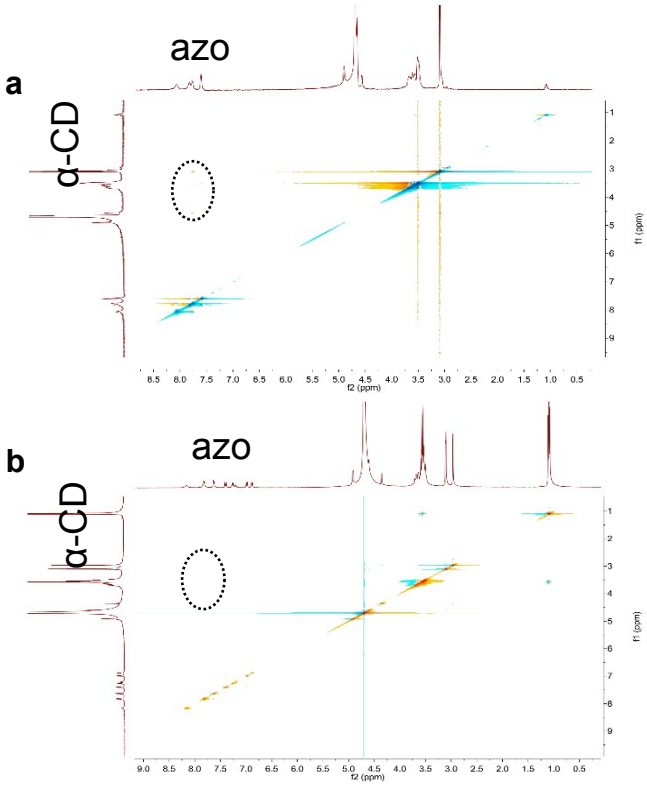

Fig. S13 ^{1}H-^{1}H NOESY spectrum of 1:1 equimolar mixture of (a) 3 mM α-CD-*E*-azo and (b) after irradiation at 365 nm for 10 min (400 MHz, D_2O, 298K).

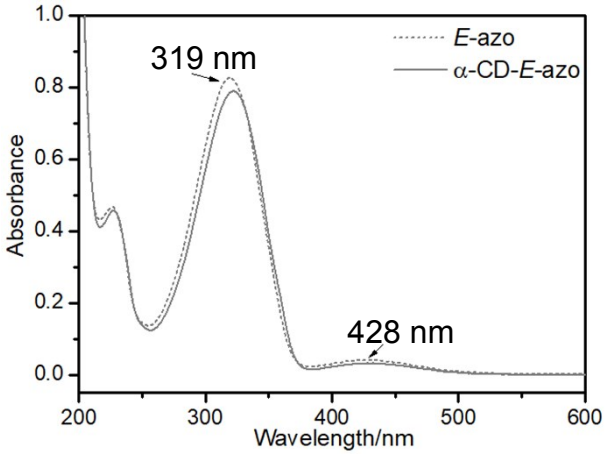

Fig. S14 The UV-Vis spectrum of *E*-azo and α-CD-*E*-azo.

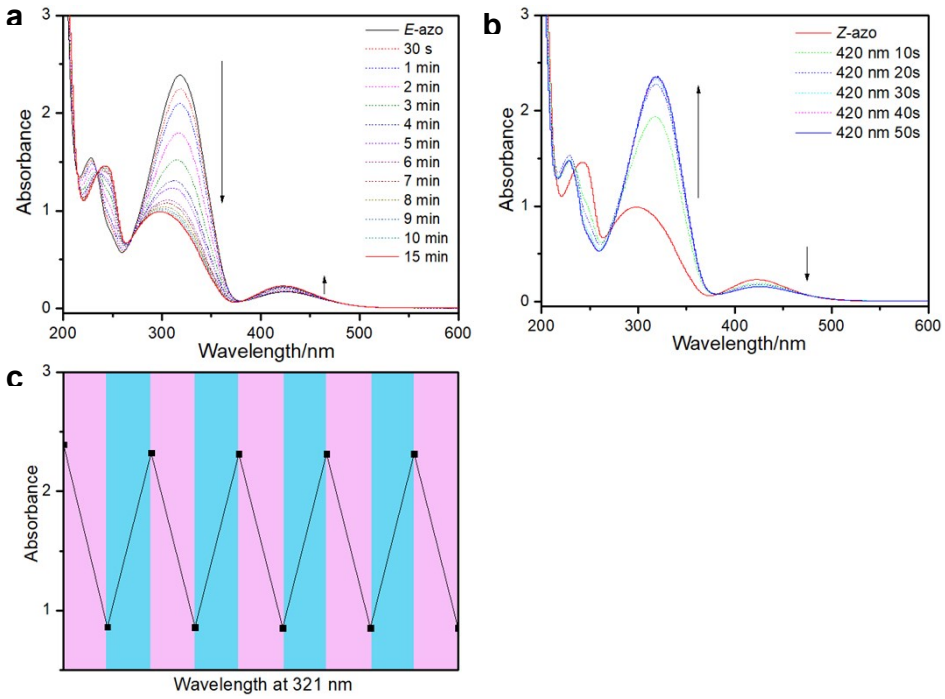

Fig. S15 UV-Vis absorption spectra of (a) *E*-azo (0.05 mM) solution under UV irradiation at 365 nm, (b) *Z*-azo after visible irradiation at 420 nm, (c) UV-Vis absorption at 321 nm of *E*-azo observed upon several cycles under irradiation at 365 nm (pink) for 10 min andirradiation at 420 nm (blue) for 1 min.

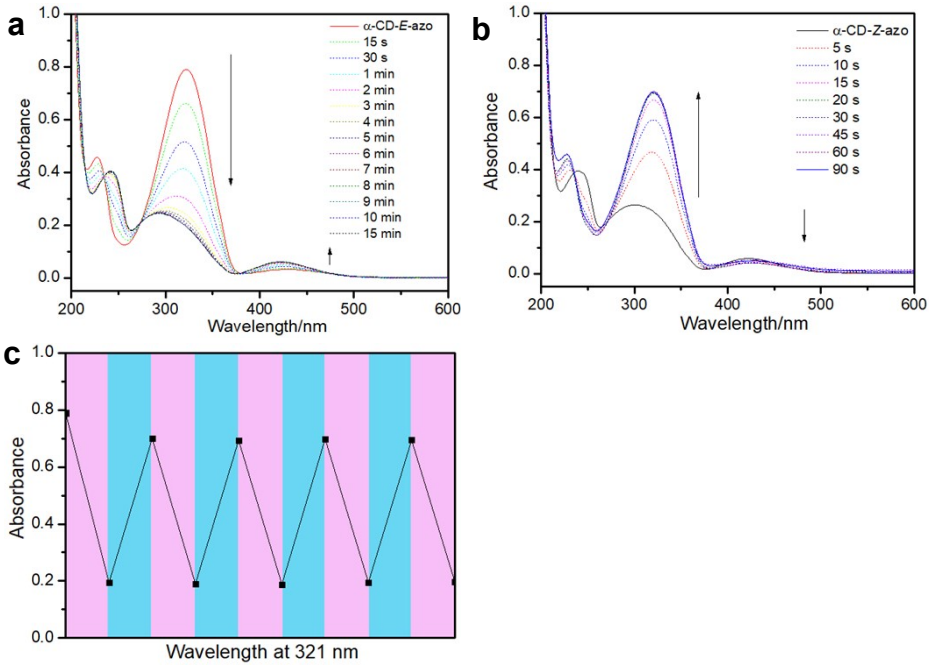

Fig. S16 UV-Vis absorption spectra of (a) α-CD-*E*-azo (0.05 mM, molar ratio, 1:1) solution under UV irradiation at 365 nm, (b) α-CD-*Z*-azo after visible irradiation at 420 nm, (c) UV-Vis absorption at 321 nm of α-CD-*E*-azo observed upon several cycles under irradiation at 365 nm (pink) for 10 min andirradiation at 420 nm (blue) for 1 min.

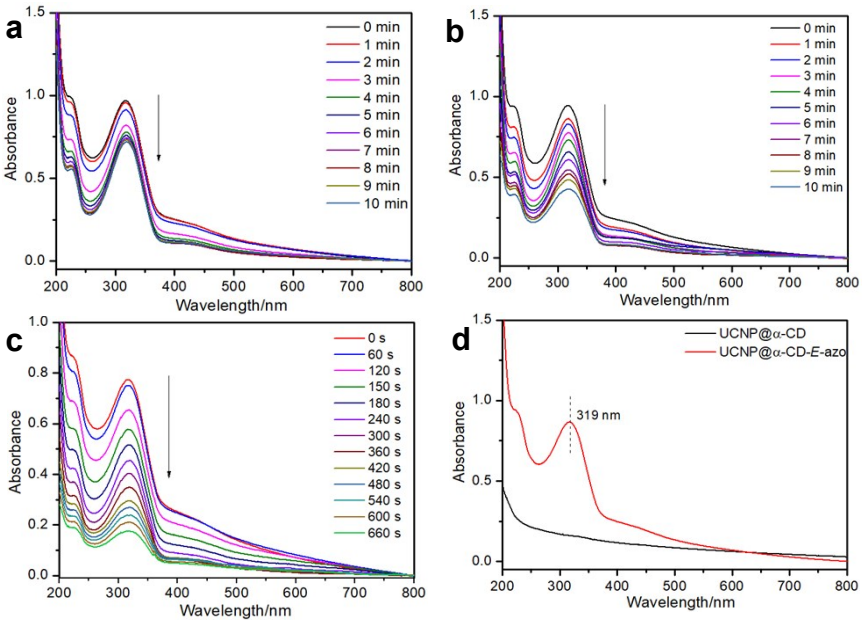

Fig. S17 UV-Vis absorption spectra of 1 mg mL^{-1} UCNP@α-CD-*E*-azo under 980 nm light irradiation at (a, b, c) 1, 2 and 3 W cm^{-2}, respectively, (d) UV-Vis absorption spectra of 1 mg mL^{-1} UCNP@α-CD and UCNP@α-CD-*E*-azo in aqueous solution.

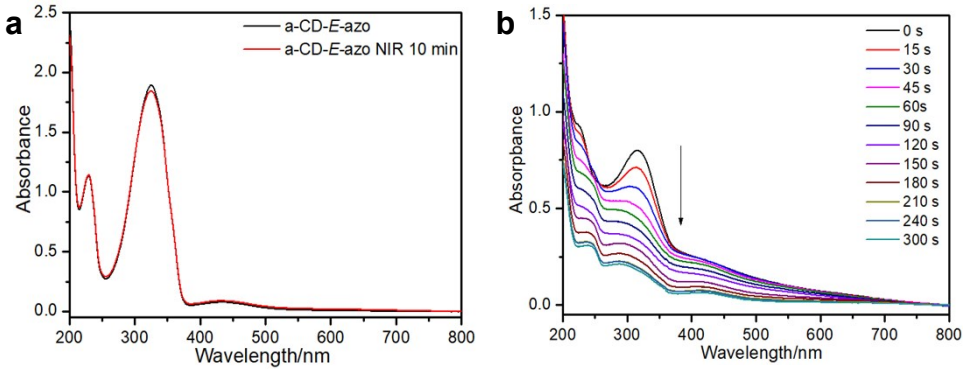

Fig. S18 (a) UV-Vis absorption spectra of 0.05 mM α-CD-*E*-azo without and with NIR light irradiation for 10 min, (b) UV-Vis absorption spectra of 1 mg mL^{-1} UCNP@α-CD-*E-azo* solution under UV light irradiation for 0-300 s.

3. The drug loading and release behaviors of SHGs

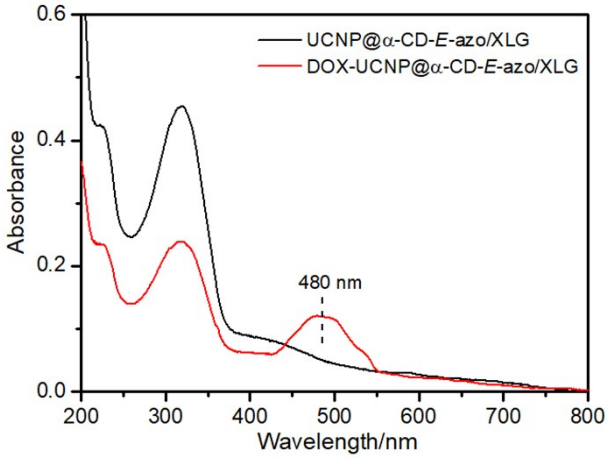

Fig. S19 UV-Vis absorption spectra of UCNP@α-CD-*E*-azo/XLG and DOX-UCNP@α-CD-*E*-azo/XLG dispersed in water.

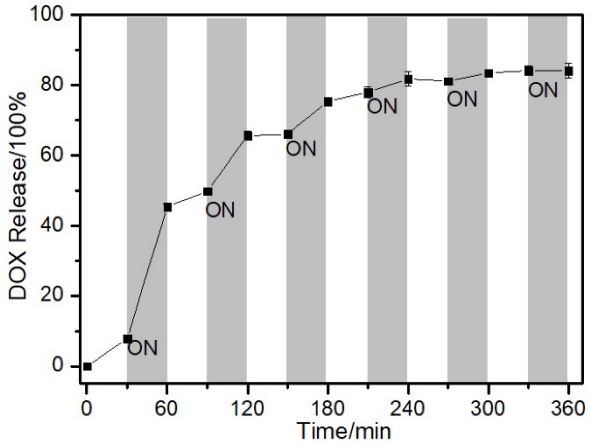

Fig. S20 DOX release from the DOX-UCNP@α-CD-*E*-azo/XLG hydrogel when switching on/off NIR nm irradiation in the dark every 30 min at pH 5.0. The NIR irradiation is 980 nm (1 W cm^{-2}).

4. The photothermal effect of SHGs

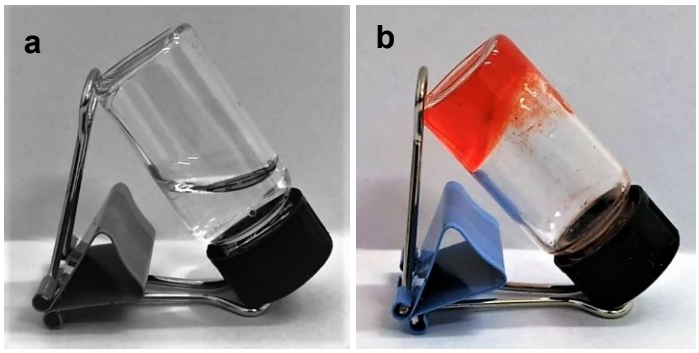

Fig. S21 (a) Digital photos of pure XLG hydrogel after external heating to 45 °C and (b) DOX-UCNP@α-CD-*E*-azo/XLG supramolecular hydrogel after external heating to 45 °C.

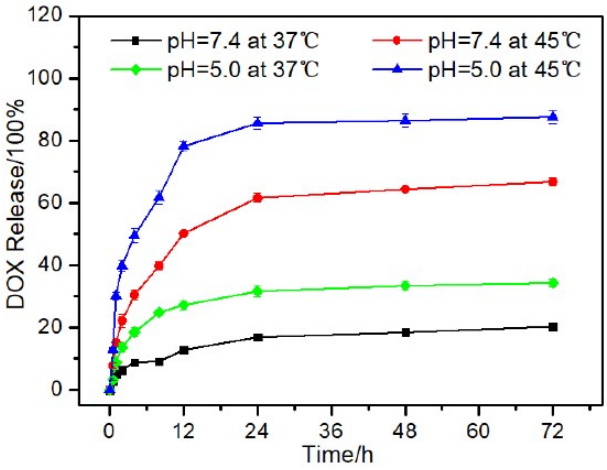

Fig. S22 The release profiles from the DOX loaded pure XLG hydrogel in pH 7.4 and pH 5.0 at different temperature under the dark, respectively.

5. In *vitro* experiment

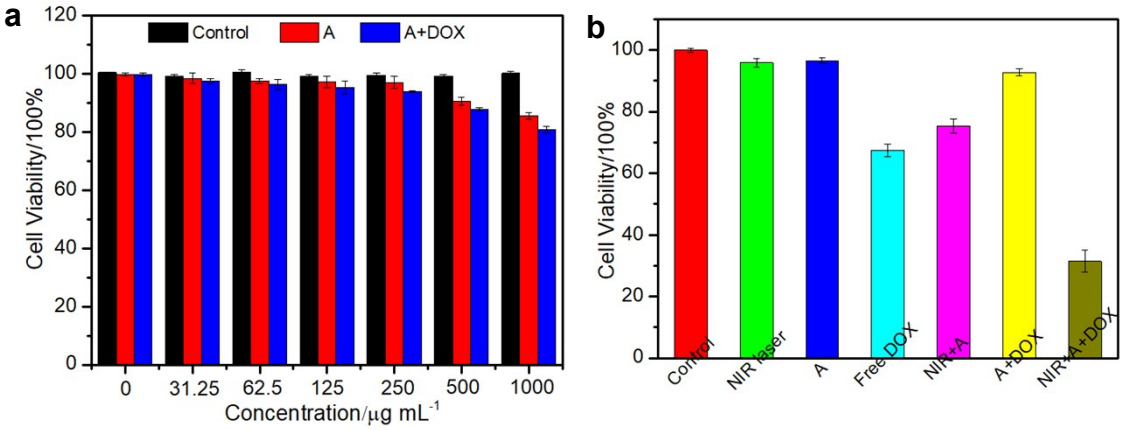

Fig. S23 (a) MTT cell viability assay of UCNP@α-CD-*E*-azo/XLG (A) and DOX-UCNP@α-CD-*E*-azo/XLG (A+DOX) hydrogels on HepG2 cells for 24 h incubation in the dark. (b) Cell viability of HepG2 cells incubated with NIR laser irradiation alone, free DOX, 250 μg mL^{-1} UCNP@α-CD-*E*-azo/XLG and DOX-UCNP@α-CD-*E*-azo/XLG without or with NIR light (980 nm, 1 W cm^{-2}) irradiation for 30 min.

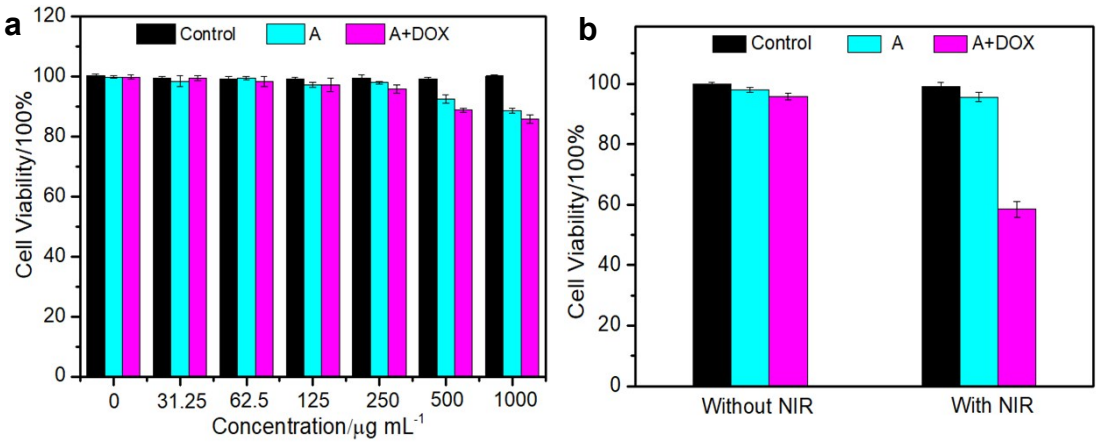

Fig. S24 (a) MTT cell viability assay of UCNP@α-CD-*E*-azo/XLG (A) and DOX-UCNP@α-CD-*E*-azo/XLG (A+DOX) hydrogels on L02 cells for 24 h incubation in the dark, (b) Cell viability of L02 cells incubated with 250 μg mL^{-1} UCNP@α-CD-*E*-azo/XLG (A) and 250 μg mL^{-1} DOX-UCNP@α-CD-*E*-azo/XLG (A+DOX) hydrogels without or with NIR light (980 nm, 1 W cm^{-2}) irradiation for 30 min.

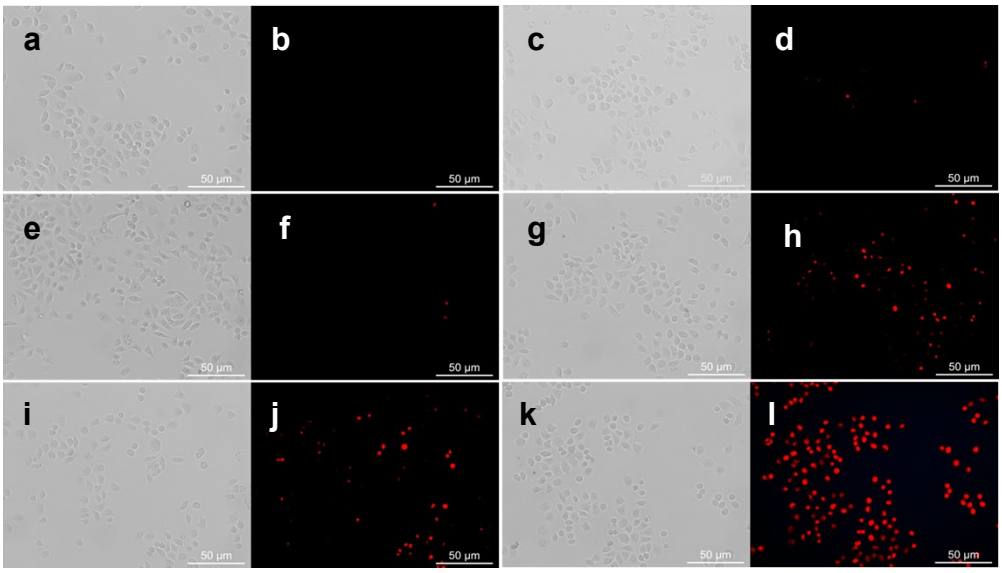

Fig. S25 (a), (c), (e), (g), (i) and (k) are the bright field images of all conditions. Fluorescence images of PI-stained HepG2 cells incubated with (b) control, (d) NIR laser irradiation alone, (f, h) 250 μg mL^{-1} UCNP@α-CD-*E*-azo/XLG and (j, l) DOX-UCNP@α-CD-*E*-azo/XLG hydrogel without or with NIR light (980 nm, 1 W cm^{-2}) irradiation for 30 min.

6. In *vivo* experiment

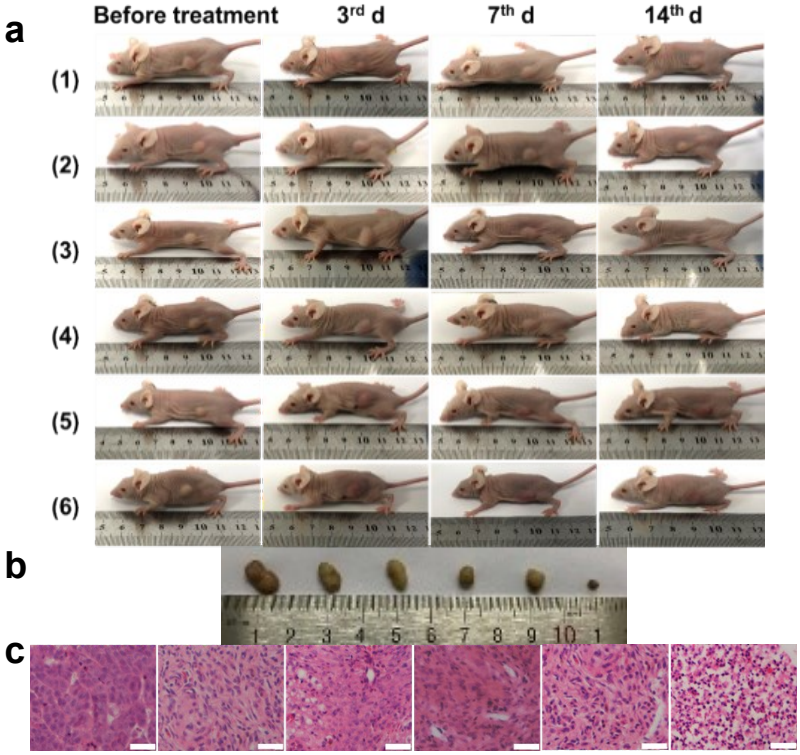

Fig. S26 (a) The typical photos of mice in groups 1-6 after various treatments. All mice were arbitrarily divided into six groups according to different experimental conditions: PBS injection only (Group 1), NIR irradiation only (Group 2), UCNP@α-CD-*E*-azo/XLG injection only (Group 3), UCNP@α-CD-*E*-azo/XLG injection plus NIR irradiation (Group 4), DOX-UCNP@α-CD-*E*-azo/XLG injection only (Group 5), and DOX-UCNP@α-CD-*E*-azo/XLG injection plus NIR irradiation (Group 6). The NIR irradiation is 980 nm (1 W cm^{-2}) for 30 min. (b) The photos of mice's tumors after various treatments. (c) Histology analysis of mice's tumor tissue in groups 1-6 at 14 th day. (Scale bar = 50 μm).

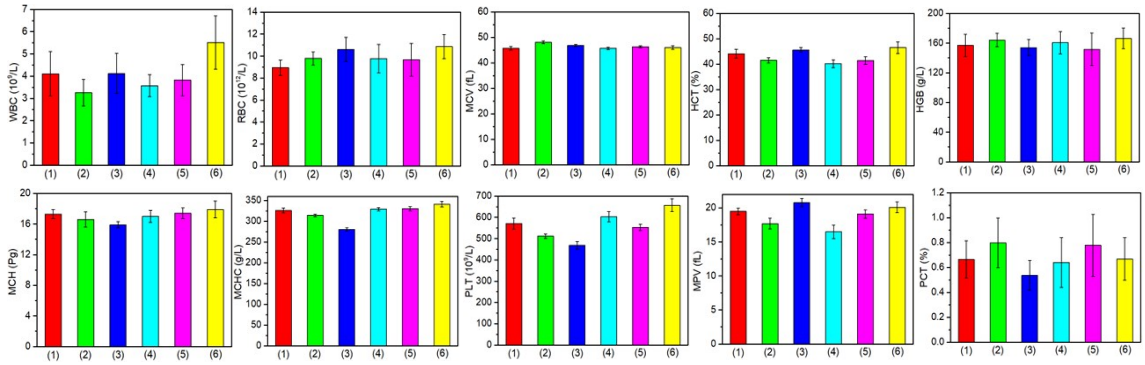

Fig. S27 The hematological data were collected from different treatments groups of mice at 14th day. Mice were randomly divided into six groups for various treatments: group 1 (PBS as control), group 2 (NIR laser irradiation for 30 min), group 3 (UCNP@α-CD-*E*-azo/XLG injection), group 4 (UCNP@α-CD-*E*-azo/XLG injection plus NIR laser irradiation for 30 min), group 5 (DOX-UCNP@α-CD-*E*-azo/XLG injection), and group 6 (DOX-UCNP@α-CD-*E*-azo/XLG injection plus NIR laser irradiation for 30 min). The NIR light laser intensity is 980 nm, 1 W cm^{-2}.